Journal of Advanced Research in Numerical Heat Transfer

Journal homepage: www.akademiabaru.com/arnht.html
ISSN: 2735-0142

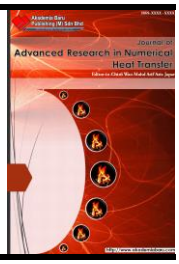

Numerical Study of Particle Behaviour in a Mixed Convection Channel Flow with Cavity using Cubic Interpolation Pseudo-Particle Navier-Stokes Formulation Method

Open Access

Ahmad Sofianuddin A. Sahak[1], Nor Azwadi Che Sidik[1,*], Siti Nurul Akmal Yusof[1], Mahmoud Ahmed Alamir[2]

[1] Malaysia – Japan International Institute of Technology (MJIIT), University Teknologi Malaysia, Jalan Sultan Yahya Petra,54100 Kuala Lumpur, Malaysia
[2] College of Science and Engineering, Flinders University, Clovelly Park, Adelaide, SA 5042, Australia

ABSTRACT

Cubic Interpolation Pseudo-Particle (CIP) method was applied to solve the hyperbolic, advective term of vorticity transport Navier-Stokes equations coupled with energy equation in the two-dimensional, incompressible and laminar flow over the cavity and Eulerian-Lagrangian approach to model the dispersion of the particles inside the cavity. Flow inside cavity with an aspect ratio (*AR*) range from 0.5 to 4, and Reynolds number (*Re*) from 50 to 1000 was investigated. Validation studies were conducted numerically by evaluating the CIP method on the flow in the channel with the cavity. Qualitative comparisons between the numerical and experimental results were evaluated and presented. Even though the presence of heat in the cavity has changed the flow structure inside the cavity due to buoyancy changes from temperature variations, it does not significantly affect the particles removal from the cavity. Furthermore, the dependency of particles dispersion on its density can also be observed. It was found that the particles with density ratio, ρ_p/ρ_f = 1.0 and 2.0 are easily affected by the flow field in the cavity compared to particles with ρ_p/ρ_f = 5.0 and 10.0. As for particles with ρ_p/ρ_f = 2.0 and 5.0, they are hardly affected by vertical flow fields resulting from inertial forces from the particles themselves. Therefore, particles tend to drag down and settle due to the gravitational force occurred instead of being removed outside the cavity. As the density ratio increased from 2.0 to 10.0, the percentage of particles removal decreased from 20% to 14%. However, the percentage of particles deposited had increased from 41% to 86%.

Keywords:
CIP method; cavity; aspect ratio; particles

1. Introduction

Cubic Interpolation Pseudo-Particle (CIP) is one of the methods for solving the general hyperbolic equation. Basically, the space within each grid is interpolated with a cubic polynomial. Therefore, both values of a particular function and its spatial derivative on the grid are predicted in advance. The primary advantages of the CIP method acquired on a compact stencil are low numerical diffusivity and high stability of the solution procedure without adapting special treatment as in Yabe and Takei [1].

Over the last few years, Takewaki *et al.,* [2]'s less diffusive CIP method has become very common to solve the hyperbolic equation. However, for spatial gradient data, the initial CIP technique using

* *Corresponding author.*
E-mail address: azwadi@utm.my

both the point values and its spatial gradients require additional border circumstances [2-5]. Usually, to get the derivation values on the node, it must distinguish the equation with the spatial variable. The procedure is not difficult for the simple case, where the velocity is constant, but it is not easy for complex equations [6].

These schemes are applied to multiple fluid flow issues, such as simulation of dam break [7-8], solitary wave [9], the dairy crown [10], shallow water equations [11-12], and fluid-structure interaction issues [13-14]. Besides, the application of CIP can be seen in other applications such as acoustic [15], geomechanics [16-17] and biomechanics [18-19]. Concerning the phenomenon of heat transfer, application of the CIP method also can be observed in several works of literature. The study of the convection process using CIP can be found in the study by Ida [20], Che Sidik *et al.,* [21] and Sheldareh *et al.,* [22].

On the numerical study of particle dispersion flow, there have been several studies reported. Kosinski *et al.,* [23] demonstrated the movement of rigid particles that suspended in a closed cavity by solving the velocity-vorticity form of Navier-Stokes equations (NSE) using Adams-Bashfort time advancement scheme for the fluid scheme. Safdari and Kim [24] using Lattice Boltzmann numerical scheme. In addition, Pratsinis and Kim [25] studied the simultaneous diffusion, thermophoresis and coagulation of submicron aerosols in non-isothermal laminar tube flows.

Eulerian-Lagrangian approach numerical scheme is based on the continuum approach for the fluid phase and Lagrangian method for the particles. In the Eulerian-Lagrangian formulation, each computational particle is considered to represent a group of particles interacting with the fluid and possessing the same features [26]. Particles dispersion behaviour depends on the characteristic of the flow within the boundaries itself. The effect of the geometrical arrangement of the boundary [27-28], heat transferred to the flow [29-32] to the particle dispersion can be observed. Combination effects of variables such as particle size, temperature difference and buoyancy effect to the particle behaviour have been studied by Feng and Michaelides [33].

On the contaminant removal, Chilukuri and Middleman [34] have modelled flow over the cavity to investigate the cleaning process. The cavity was modelled to represent the roughness of the surface with different geometry and shape. Besides, it also represents transport components which are poorly fitted and junction [35-36], which may be resulting in the contaminant trapped between the surfaces. The effect of fluid flow on the removal of dissolution substance from small cavities with different shape and geometry were studied by previous researchers [37-39]. Furthermore, investigation on the effect of mixed convection to the effectiveness of removal also had been studied [21,32, 40-41]. Uses of particles as a contaminant in the cavity to study the cleaning process has been considered [21,32] to gain the understanding of particle behaviour inside the cavity due to its broad application in engineering and natural studies.

The governing equations of the interactions between fluid-particle flow have been developed and established for many decades. In most applications, this flow did not stand alone as the fluid-particle flow itself. It often interacts with various phenomena such as heat transfer, deposition and evaporation, adding the complexity to understand the physics of the flow. Thus, the equations governed must suit to the specific cases before further analyses can be done. Recent advancements in computational capabilities, including the development of robust numerical algorithms, provide opportunities for researchers to investigate these problems. However, researchers must define the physical model for both fluid and particle before a simulation can be done. Thus, setting physical model requires researchers to select the suitable numerical method that gives an accurate and stable solution, within the boundary defined. A little is known about the application CIP in the development of fluid flow phase algorithm in such specific cases of particle behaviour in the channel with the cavity that is dependent on various variables. CIP method is arguably one of the numerical techniques that

provides a solution with higher accuracy and less diffusivity compared to other numerical methods. Therefore, by developing a single particle-laden flow algorithm combining the CIP method for fluid phase with the particles-phase may beneficial to scientists or engineers to obtain a stable and accurate solution for related problems.

Based on the brief review on the literature above, there is no detail discussion on utilizing a combination of CIP numerical scheme to assess the flow in a channel with cavity with the particle dispersion and the combining effect of different geometrical and fluid parameters with the presence of heat. Motivated with these studies, this research analyzes the particle behaviour in the cavity of a channel with a heated cavity using the numerical algorithm based on the established CIP methods.

This study aims to investigate the effect of mixed convection of heat in the cavity to the flow structure at various combinations of geometrical and flow parameters. Therefore, this research focuses on the coupling of particle-laden flows with heat transfer. This could provide a better understanding of complex interactions of fluid and particle with other physical phenomena for specific engineering application which is material transportation, hydrodynamic cleaning and sedimentation process in the cavity.

2. Methodology

2.1 Experimental Setup

Figure 1 illustrates an overview of the experimental layout. The experiment has been conducted in a closed-circuit water channel, which consists of a tank, that acts as the reservoir, centrifugal pump, two valves, flow meter, to indicate the flow rate and also the closed water channel, made with 4 mm thick acrylic material with different cavity aspect ratios that were specially designed for this experiment.

The entrance length (L_e) is defined as the region where the viscous effects near the wall affect the velocity profile of the flow, which changes constantly [42]. Therefore, it is important to determine the entrance length of the upstream flow so that the velocity profile of the incoming flow becomes constant before reaching the cavity and so as not to affect the flow formed in the cavity.

The length of the entrance, L_e for laminar flow can be written in a function of Reynolds number, Re as follows

$$L_{\mathrm{e}} = 0.06 Re D_h \tag{1}$$

where Re = Reynolds number and D_h = hydraulic diameter of the pipe. However, because the pipe is not circular, the hydraulic diameter can be described as

$$D_h = 4A/P \tag{2}$$

where A is the area of the cross-section and P is the perimeter of the wet part of the pipe. From Eq. (1), L_e for different Re has been calculated and presented in Table 1.

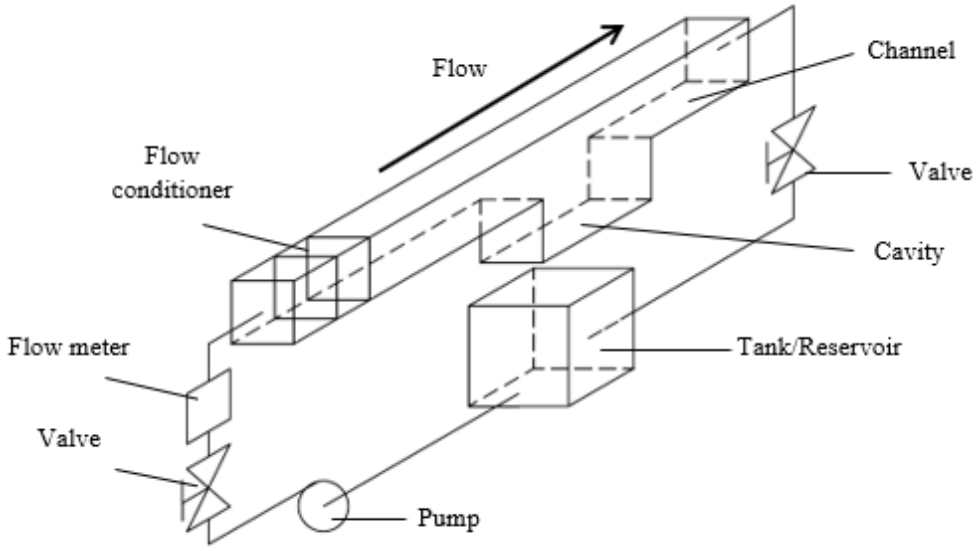

Fig. 1. Diagram of the experimental layout and its component

Table 1
Length of the entrance, L_e required for each of Reynolds number, Re

Reynolds number, *Re*	100	400	1000
Entrance length, L_e(mm)	150	600	1500

The test section consists of a smooth 25 × 25 mm square channel with 1500 mm long inlet (L_i), 500 mm long outlet (L_o) and a wall thickness of 4 mm for the whole channel and cavity as Figure 2. For cavity section, the length and depth (*L* and *H*) are the same with the channel opening (25 mm) but have a variable range of length, *L* from 75 to 100 mm (*AR* = 3 and 4). Summary of test section dimension was shown in Table 2.

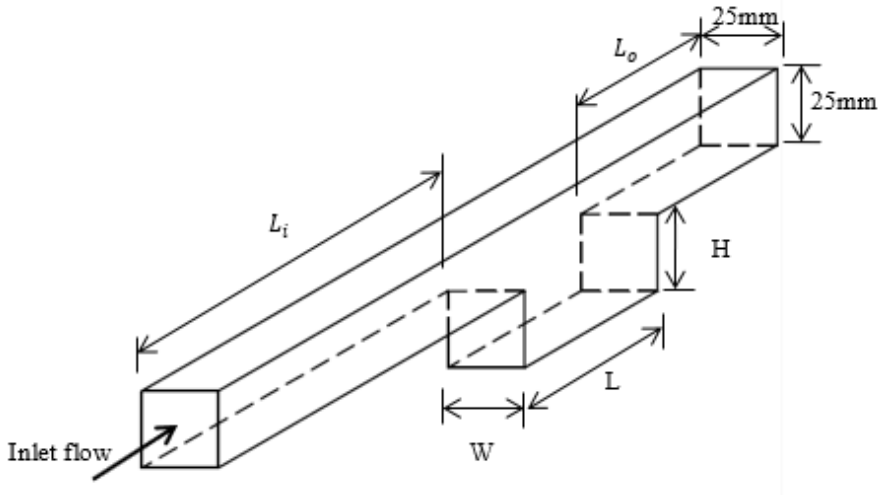

Fig. 2. Cavity channel geometric parameters

Table 2
Summary of test section dimension

Aspect Ratio (*AR*)	L_i(mm)	L_o (mm)	*L* (mm)	*W* (mm)	*H* (mm)
4	1500	500	100	25	25
3	1525	500	75	25	25

There are two different sizes of cavities used in this experiment to represent two different aspect ratio (*AR*) which is 3 and 4. Other than comparison purpose to the numerical results within the research scopes, AR 3 and 4 were selected because longer cavity's length provides a clear image for visualization. Shorter length affecting the diffusion rate of the dye used for visualization, thus, produce an unclear image of flow structure. For each case, three different Reynolds number, *Re* have been used, 100, 400 and 1000. These values have been selected so that it can be compared with numerical results from the present method and works of literature within the scopes of the research. The Reynolds number, *Re* is calculated from the incoming flow average velocity (u_{avg}), the hydraulic diameter of the channel, D_h and kinematic viscosity of the fluid, υ. By definition,

$$Re = \frac{u_{avg} D_h}{\upsilon} \tag{3}$$

By controlling the flow rate of the incoming flow, we can adjust to the desired velocity of the flow and therefore, controlling Reynolds number, *Re* of the flow as well. Using Eq. (3), for Reynolds number, *Re* from 100 to 1000, calculated range of flow velocity, u_{avg} in the channel between 4.016 mm/s and 40.160 mm/s. Determination of u_{avg} for each *Re* is important in order to obtain the value of flow rate required for the experiment. The flow rate value can be obtained by using Eq. (4).

$$Q = u_{avg} A \tag{4}$$

where Q is the flow rate, u_{avg} is the average flow velocity and A is the area of the channel cross-section. This is crucial as the range of flow rate, Q value needed for suitable pump and flowmeter scale selection. The flow rate based on the high-velocity range is between 0.151 *l*/min and 1.506 *l*/min. The summary of flow rate for each *Re* is shown in Table 3.

Table 3
Flow rate and flow with corresponding Reynolds number, *Re*

Reynolds number, *Re*	Average flow velocity, u_{avg} (mm/s)	Flow rate, Q (*l*/min)
100	4.0160	0.151
400	16.064	0.602
1000	40.160	1.506

In the experiment, the flow rate was controlled by using a ball valve positioning upstream the pump and measured by glass flowmeter, Platon NG series range from 0.1 *l*/min-1.5 *l*/min with accuracy up to 1.25% full-scale deflection (FSD).

2.2 Flow Visualization

Three methods were used to visualize flows in experimental fluid dynamics which are surface flow visualization, particles tracer method and optical method [43-45]. In this study, the classical flow visualization technique using liquid dye as used by Mega *et al.,* [46] was chosen. This is due to the limit of the qualitative aspect of the flow structure. Liquid dye technique can determine the moving

instability of the shear layer past over the cavity. This method, however, has a drawback. It cannot produce excellent quality images for stationary vertical structure for Reynolds number, Re below 100 and aspect ratio, *AR* less than 2 for this experiment configuration.

The experiment is using Sony alpha 6000 (α6000), ILCE6000 model, 24 megapixels mirrorless digital camera with 16-55 mm zoom lens as image recorded device and positioned in front of cavity to visualize the velocity profile and flow behaviour with different Reynolds number, Re especially in the cavity. The experiments for each Reynolds number were repeated three times to obtained reliable and consistent visual results. The reproducibility of flow visualizations was verified by recording various picture sequences with a different channel running, and by testing different dye ink-water mixture. Note that there is a saturation of the cavity with ink if the observation time is too long. Therefore, the dynamical flow structure in the cavity cannot be identified.

2.3 The Numerical Scheme

Advection equation for hyperbolic type of equation can be solved by using Cubic Interpolated Pseudo-particle (CIP) method. This method is a semi-Lagrangian scheme which gives not an only less diffusive result but also stable outcome without any flux limiter [47]. Therefore, Yabe [4, 47] proposed a general hyperbolic solver. The solver scheme needs to split the equation into two parts which are advection and non-advection phases.

Eqs. (5) and (6) show the vorticity transport and energy equation in dimensionless form. The equations consist of advection and non-advection part on the left- and right-hand side of the equations, respectively. The non-advection phase of the equations will be solved by using central finite difference, and the advection phase will be solved using two-dimensional CIP approach.

Momentum dimensionless equation

$$\frac{\partial \Omega}{\partial \tau} + U\frac{\partial \Omega}{\partial X} + V\frac{\partial \Omega}{\partial Y} = \frac{1}{Re}\left(\frac{\partial^2 \Omega}{\partial X^2} + \frac{\partial^2 \Omega}{\partial Y^2}\right) + \frac{Gr}{Re^2}\frac{\partial \theta}{\partial X} \tag{5}$$

Energy dimensionless equation

$$\frac{\partial \theta}{\partial \tau} + U\frac{\partial \theta}{\partial X} + V\frac{\partial \theta}{\partial Y} = \frac{1}{PrRe}\left(\frac{\partial^2 \theta}{\partial X^2} + \frac{\partial^2 \theta}{\partial Y^2}\right) \tag{6}$$

where Ω is dimensionless vorticity, X and Y are dimensionless space in horizontal and vertical direction respectively, U and V are dimensionless velocity component in horizontal and vertical direction respectively, Gr is Grashof number, Re is Reynolds number, θ is dimensionless temperature, τ is dimensionless time, and Pr is Prandtl number. In conjunction with the CIP method, Eq. (5) divided into advection and non-advection phases. Then, the split equation must be differentiated to determine the Ω and θ gradient. Thus, the differentiation results are described as the following equation.

The advection phase:

Momentum

$$\frac{\partial \Omega}{\partial \tau} = -\left(U\frac{\partial \Omega}{\partial X} + V\frac{\partial \Omega}{\partial Y}\right) \tag{7}$$

$$\frac{\partial_X \Omega}{\partial \tau} = -\left(U\frac{\partial_X \Omega}{\partial X} + V\frac{\partial_X \Omega}{\partial Y}\right) \tag{8}$$

$$\frac{\partial_Y \Omega}{\partial \tau} = -\left(U\frac{\partial_Y \Omega}{\partial X} + V\frac{\partial_Y \Omega}{\partial Y}\right) \tag{9}$$

Energy

$$\frac{\partial \theta}{\partial \tau} = -\left(U\frac{\partial \theta}{\partial X} + V\frac{\partial \theta}{\partial Y}\right) \tag{10}$$

$$\frac{\partial_x \theta}{\partial \tau} = -\left(U\frac{\partial_x \theta}{\partial X} + V\frac{\partial_x \theta}{\partial Y}\right) \tag{11}$$

$$\frac{\partial_Y \theta}{\partial \tau} = -\left(U\frac{\partial_Y \theta}{\partial X} + V\frac{\partial_Y \theta}{\partial Y}\right) \tag{12}$$

and the non-advection phase

Momentum

$$\frac{\partial \Omega}{\partial \tau} = \frac{1}{Re}\left(\frac{\partial^2 \Omega}{\partial X^2} + \frac{\partial^2 \Omega}{\partial Y^2}\right) + \frac{Gr}{Re^2}\frac{\partial \theta}{\partial X} \tag{13}$$

$$\frac{\partial_X \Omega}{\partial \tau} = \frac{1}{Re}\left(\frac{\partial^3 \Omega}{\partial X^3} + \frac{\partial^3 \Omega}{\partial X \partial Y^2}\right) - \partial_X \Omega\frac{\partial U}{\partial X} - \partial_Y \Omega\frac{\partial V}{\partial X} + \frac{Gr}{Re^2}\partial_X \frac{\partial \theta}{\partial X} \tag{14}$$

$$\frac{\partial_Y \Omega}{\partial \tau} = \frac{1}{Re}\left(\frac{\partial^3 \Omega}{\partial X^2 \partial Y} + \frac{\partial^3 \Omega}{\partial Y^3}\right) - \partial_X \Omega\frac{\partial U}{\partial Y} - \partial_Y \Omega\frac{\partial V}{\partial Y} + \frac{Gr}{Re^2}\partial_X \frac{\partial \theta}{\partial Y} \tag{15}$$

Energy

$$\frac{\partial \theta}{\partial \tau} = \frac{1}{PrRe}\left(\frac{\partial^2 \theta}{\partial X^2} + \frac{\partial^2 \theta}{\partial Y^2}\right) \tag{16}$$

$$\frac{\partial_X \theta}{\partial \tau} = \frac{1}{PrRe}\left(\frac{\partial^3 \theta}{\partial X^3} + \frac{\partial^3 \theta}{\partial X \partial Y^2}\right) - \partial_X \theta\frac{\partial U}{\partial X} - \partial_Y \theta\frac{\partial V}{\partial X} \tag{17}$$

$$\frac{\partial_Y \theta}{\partial \tau} = \frac{1}{PrRe}\left(\frac{\partial^3 \theta}{\partial X^2 \partial Y} + \frac{\partial^3 \theta}{\partial Y^3}\right) - \partial_X \theta\frac{\partial U}{\partial Y} - \partial_Y \theta\frac{\partial V}{\partial Y} \tag{18}$$

where $\partial_X \Omega = \partial\Omega/\partial \mathrm{X}$ and $\partial_Y \Omega = \partial\Omega/\partial \mathrm{Y}$, $\partial_X \theta = \partial\theta/\partial \mathrm{X}$ and $\partial_Y \theta = \partial\theta/\partial \mathrm{Y}$. The details description of the advection and non-advection phase is documented in [48] and will not be given here.

2.4 Fluid-Particle Interaction

There are two types of movement in particulate flows which are translational motion and rotational motion. To describe the motion of an individual particle, Newton's second law of motion can be used as in Zhu *et al.,* [49]. For the translational and rotational movement of particle i with mass m_i and moment of inertia I_i , the governing equation can be described as

$$m_i \frac{dv_i}{dt} = \sum_j F_{ij}^c + \sum_k F_{ik}^{nc} + F_i^f + F_i^g \tag{19}$$

$$I_i \frac{d\omega_i}{dt} = \sum_j M_{ij} \tag{20}$$

where ω_i and v_i are the angular and translational velocities of particle *i*, respectively, M_{ij} and F_{ij}^c are the torque and contact force acting on particle *i* by particle *j* or walls, F_{ik}^{nc} is the noncontact force acting on particle *i* by particle *k* or other sources, fluid-particle interaction force on particle *i*, is represented by F_i^f and F_i^g is the body force of the particle, gravity.

Since no non-contact forces were considered in the present research and the particles were assumed with no rotational motion applied, the governing equation for particles can be described as

$$m_i \frac{dv_i}{dt} = \sum_j F_{ij}^c + F_i^f + F_i^g \tag{21}$$

F_i^f which is mainly the drag force acting on the particle, can be described as follows

$$F_i^f = F_d = 1/2\rho_f C_D A_P |u_i - v_i|(u_i - v_i) \tag{22}$$

where ρ_f is the density of the fluid, A_P is the area of the particle projected on a plane normal to the flow direction, C_D is the drag coefficient and u_i and v_i are the velocities of the continuous fluid phase and particle phase. The C_D is primarily a function of Reynolds number, Re, defined as

$$Re_p = (\rho_f D_p |u_i - v_i|)/\mu \tag{23}$$

where μ is the dynamic viscosity of the fluid and D_p is the particle diameter. Since the value of Re here is based on the value of relative velocity between the particle and the fluid, Re_p the notation is used to distinguish between the flow's Reynolds number, Re. In the present research, the value of C_D can be determined as follows [50]

$$C_D = \frac{24}{Re_p} \quad \text{for } Re_p < 1 \tag{24}$$

$$C_D = \frac{24}{Re_p}\left(1 + \frac{3}{16}Re_p\right) \quad \text{for } 1 < Re_p < 5 \tag{25}$$

$$C_D = 1 + \frac{{Re_p}^{2/3}}{6} \quad \text{for } Re_p < 1000 \tag{26}$$

On the other hand, F_i^g can be expressed as follows

$$F_i^g = \left(1 - \frac{\rho_f}{\rho_p}\right) g \tag{27}$$

where ρ_f is the working fluid density, ρ_p is particle density and g is the gravitational acceleration. Therefore, by getting previous information, the velocity and the position of the particles can be obtained by solving equation (3.03) using the fourth-order Runge-Kutta method. The detailed solutions have been discussed in Arman and Kim [24].

2.5 Validation Study

2.5.1 Fluid particle interaction

The validation study of the behaviour of single-particle inside the cavity flow was carried out by comparing present results with the experimental research done by Tsorng *et al.,* [51] and numerical study by Kosinski *et al.,* [23]. Tsorng *et al.,* [51] studied the behaviour of a single particle suspended in a lid-driven cavity flow. The experiment setup includes fluid with specific gravity 1.21 and kinematic viscosity of 37.2 mm^2/s and, within a cavity with 10 cm sidewall. The particle has the density almost similar to the working fluid. The lid was moving with a velocity of 17.5 cm/s. This information matched the Reynolds number, Re = 470 [23].

The computational domain was set up, as shown in Figure 3. The numerical domain of the cavity had the aspect ratio, *AR* = 1, where *L* = *H* =1. The grid points used is fixed to 101 x 101. The particle properties for the validation study were obtained from work by Arman and Kim [24] as they also conducted the comparative analysis for validation of single-particle behaviour in the driven cavity using the results from Tsorng *et al.,* [51] and Kosinski *et al.,* [23]. Table 4 shows the spatial resolutions generated for the study and the parameters involved.

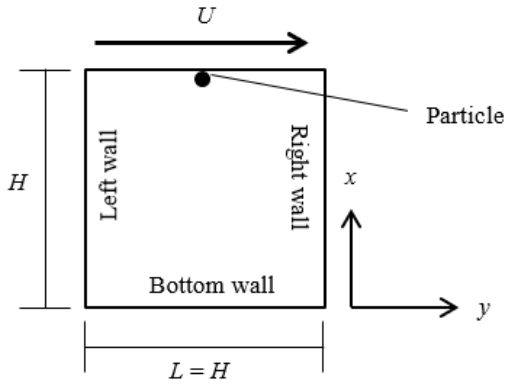

Fig. 3. Computational domain's schematic diagram and boundary conditions for validation study in lid-driven cavity of trajectory of single particle in lid-driven cavity

Table 4
Resolution of mesh and parameters used for the fluid-particle interaction validation study

Depth (*H*) and length (*L*) of the domain	No. of grid points, (*i* x *j*)	Cell size ($\Delta X \times \Delta Y$)	Dimensionless time step, $\Delta\tau$	Particle density ratio, ρ_p/ρ_f	Particle size, D_p
H = *L* = 1	101 x 101	0.01 × 0.01	0.0001	1.0	0.001

3. Results

3.1 Validation Numerical Results of Mix Convection

The computational analysis of the two-dimensional, laminar mixed convective flow of air (Prandtl number, Pr = 0.7) over open-ended cavity for aspect ratio, AR = 1 using CIP method were performed. The flow Reynolds number, Re was fixed to 100, but the velocity and temperature distribution of the buoyancy forces can be affected by varying the Richardson number (Ri), ranging from 0.1 to 10.0. Throughout the investigation, the numerical results of mixed convection are compared and evaluated with work by Manca *et al.,* [52], Abdelmassih *et al.,* [53] and Stiriba *et al.,* [54].

3.1.1 Effect of Richardson number, Ri on the flow streamline and thermal fields inside the cavity

For all value Richardson number, Ri, Figure 4(a) shows a single formation of vortex existed within the cavity using the thermal CIP numerical method. For Ri = 0.1, buoyancy effect in the cavity at this condition is insignificant as the dominant diffusion heat transfer process takes places. The isotherms (Figure 5) within the cavity indicate that heat transfer via conducting is dominant. It governed by diffusion through the flow field and by the weak circulating flow.

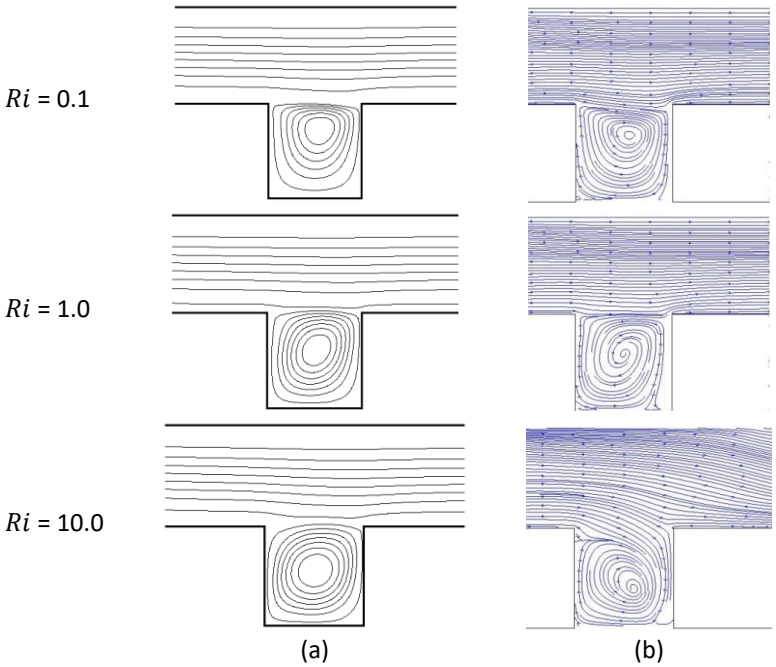

Fig. 4. Streamlines and vortex formation comparisons for *AR* = 1, Re = 100 from (a) present results, (b) Abdelmassih *et al.,* [53]

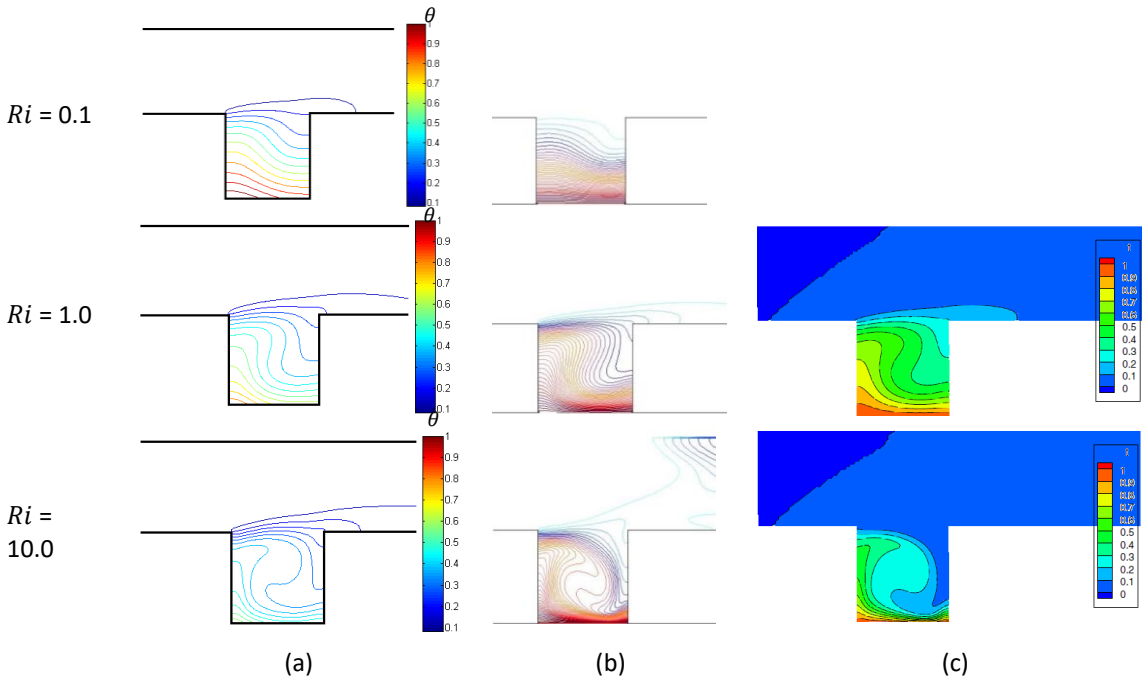

Fig. 5. Isotherm lines comparisons for *AR* = 1, Re = 100 from (a) present results, (b) Abdelmassih *et al.,* [53] and (c) Stiriba *et al.,* [54]

As the Richardson number, *Ri* increase to 1.0, the center of the flow circulation is slightly shifted to the center of the cavity. Besides, the shape of the flow circulation skewed becoming oval-shaped. This is because the buoyancy force becomes stronger. In addition, convective heat transfer becomes more dominant and as *Ri* increase to 10.0, the heat transfer within the cavity occurs prominently via convection. At this point, natural convection dominated the process of heat transfer. The changes in the flow structure inside the cavity are mostly due to the density variation to the temperature distribution, θ inside the cavity rather than the shear itself. It can be seen by the non-linear isotherms that become significant within the cavity. The convection process inside the cavity is affecting the flow circulation, thus, affecting the velocity of the flow as shown in Figure 5. However, the result in flow circulation is slightly different compared to Abdelmassih *et al.,* [53]. Their results show that the induced flow penetrated the cavity and center of the circulation drift to the lower half of the cavity. In contrast, the present only indicates that the circulation is getting bigger as the buoyancy forces getting stronger. In addition, it clearly shows that no penetration from the external flow into the cavity.

3.2 Numerical Study of Particle Behaviour in a Mixed Convection Channel Flow with Cavity

The aspect ratio, AR = 1 using the CIP method was chosen to analyze the particle behaviour in a mixed convection channel flow with the cavity. On the presence of heat along the bottom wall, an observation was made to the effect of the heat on the flow circulation inside the cavity. From the observation, there are slightly change in streamline were recorded. The changes are higher for small Reynolds number, Re = 50 compared to larger Re. The convection of the heat process in the cavity changes from forced convection to natural convection as Gr increases from 1000 to 4000. The changes of flow pattern are encountered due to stronger buoyancy effect as *Gr* increases. The buoyancy forces from the convection affect the strength of the vortex inside the cavity as the velocity increases as shown in Figure 6(a). From the figure, there are increases in velocity of about 72.4% and 55.7% on maximum and minimum *V*-velocity as Gr increases from 1000 to 4000.

As Reynolds number, Re increases to 100, there is a main circulation developed filled inside the cavity, and the shape of their streamlines varies at various *Gr*. However, the changes of vortex shape inside the cavity are lesser as the Gr increases from 1000 to 4000, as illustrated in Figure 7(a). For temperature, θ contour, it can be seen in Figure 7(b) that *Gr* values affect the temperature distribution. Furthermore, forced convection from the flow is dominating the heat transfer inside the cavity and buoyancy force have a smaller effect on the flow compare to Re = 50 due to higher inertial forces from the flow. The presence of heat in the flow inside the cavity slightly influences the behaviour of the dispersion of the particles. The effect of heat on the dispersion of the particles will be discussed later.

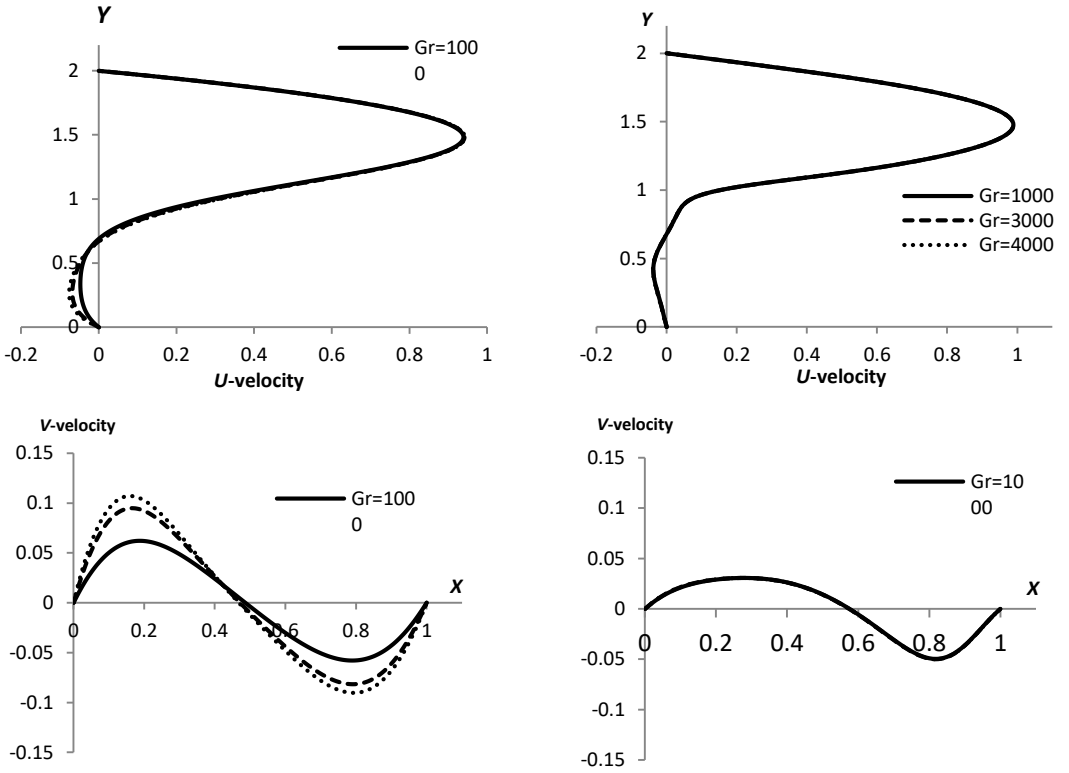

Fig. 6. Comparison of the velocity profile of horizontal (top) and vertical component (bottom) along the centerline of the cavity with aspect ratio, *AR* = 1 at different Grashof number, Gr for (a) Re = 50 and (b) Re = 1000

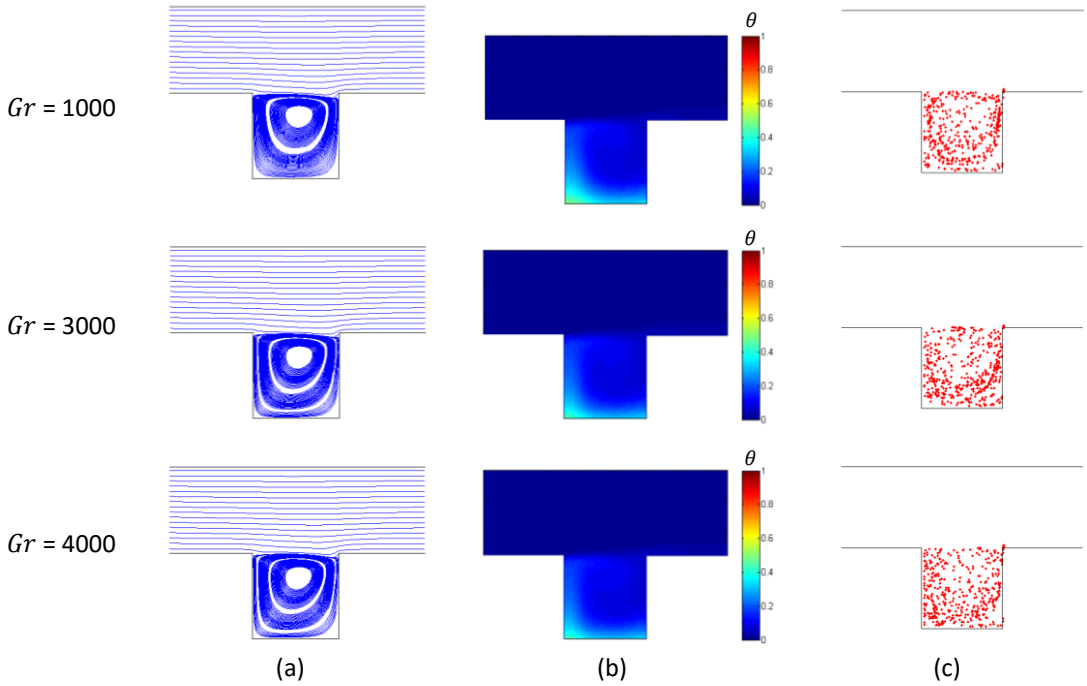

Fig. 7. Flow structure (a) temperature (b) and particle distribution (c) in the flow field of the channel with cavity with aspect ratio, *AR* = 1 at steady state at Reynolds number, Re = 100 at various Grashof number, Gr

However, the changes of flow structures are almost insignificant at Re = 1000 for all Gr value as shown in Figure 8(a). As the convection process in Re = 1000, forced convection also dominating the heat transfer inside the cavity. The phenomena can be observed as the heat from the cavity transferred to the flow circulation mostly by the advective process, thus, translated by temperature, θ contour as shown in Figure 8(b). In this process, inertial forces of the flow circulation are dominant from buoyancy forces; thus, changes of Gr from 1000 to 4000 did not significantly change the flow behaviour. Therefore, no significant differences in the velocity of the flow circulation recorded, as shown in Figure 6(b).

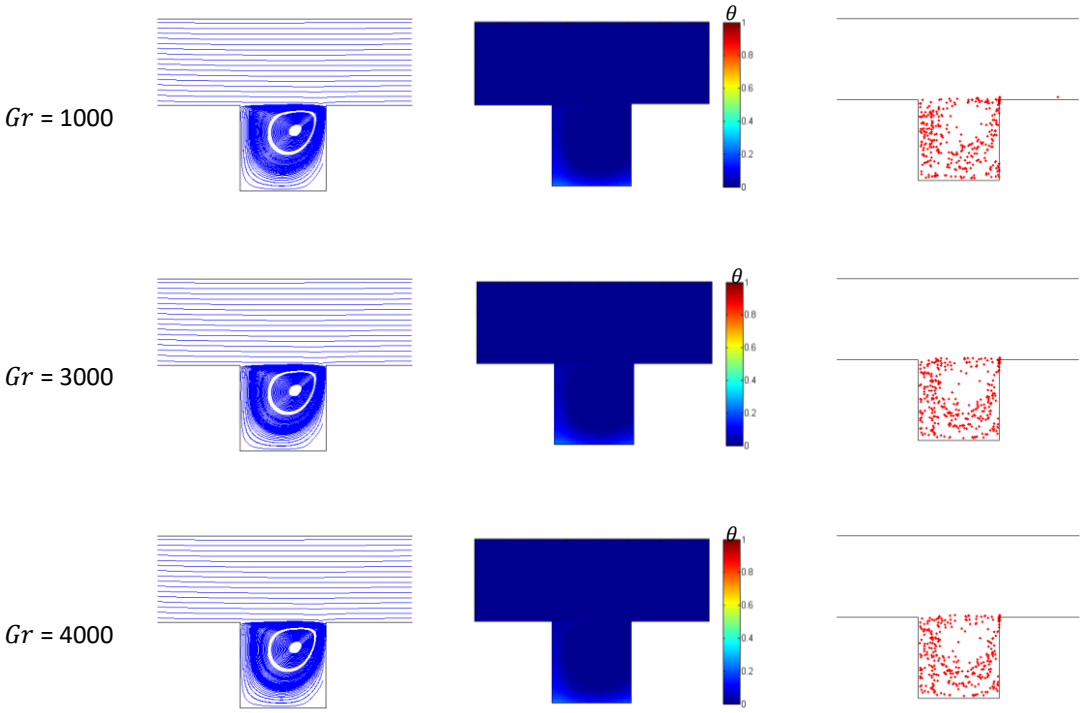

Fig. 8. Flow structure (a) temperature (b) and particle distribution (c) in the flow field of the channel with cavity with aspect ratio, *AR* = 1 at steady state at Reynolds number, Re = 1000 at various Grashof number, Gr

3.3 Effect of Heat on The Dispersion of Particles Removal Process

Figure 9 show percentages of particle removed for a cavity with AR = 1, 2 and 4 at various Reynolds number, Re and Grashof number, Gr. By focusing on the effect of heat on the particles removal process, generally, there are no significant changes to the percentages. Details changes in removal percentages presented in Figure 9 for all aspect ratio, *AR* of the cavity. For *AR* = 1, the percentages decreasing for all Re as Gr increasing from 1000 to 4000. For Re = 50, the percentage decrease from 13.9% to 12.4% while for Re = 100, the percentage slightly decrease from 11.6% to 11.2%. For Re = 1000, the percentage decrease from 21.2% to 19.6%. For Re = 1000, the percentage of removal has shown an increase from 39% to 39.2% as Gr increases from 1000 to 3000 before decreasing to 39% for Gr = 4000. However, there are increases in percentage for Re = 1000. The percentage decrease from 81.4% to 80.6% as Gr increases from 1000 to 3000 before the percentage jump to 84.4% for Gr = 4000.

Notably, for Re = 100, the particles seem to disperse along with the higher velocity and vorticity region inside the cavity as shown in Figure 7(c) regardless the value of Gr as discussed in previous work by Brandon and Aggarwal [55] and Jafari *et al.,* [56]. As Re increases to 1000, the strength of the vortices increases. As a result, the cloud of particles moved from the middle of the cavity and rotates along the peripheral of the vortex due to the inertia of the particles [24] as shown in Figure 8(c). Insignificant changes in particles removal percentage for different Gr seems to be debatable to the heat and mass transfer discussion by Fang [42] especially for *Re* = 50. Combination of buoyancy force and flow inertia supposed to increase the removal percentage significantly. This contradiction may be due to the absence of particles consideration on the analysis of fluid removal from the cavity by Fang [42]. Since the particles used in the present study need to consider the interaction between itself and the walls; therefore, the results may differ from expected. Besides, parameters of the particles should be taken into account for the differences.

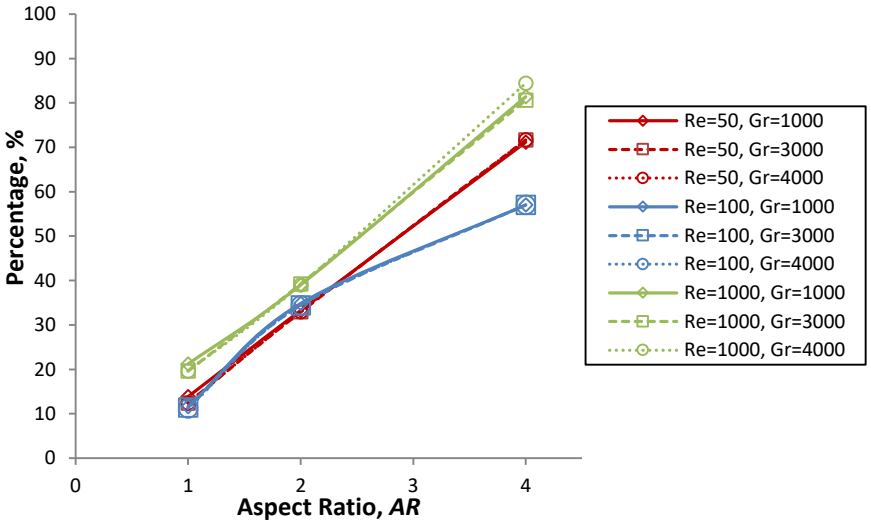

Fig. 9. Percentage of particles removal at various Reynolds number, Re at different Grashof number, Gr for a cavity at various aspect ratio, *AR*

3.4 Effect of Different Density Ratio, ρ_p/ρ_f to the Dispersion of Particles Removal Process

Figure 10 presents the percentage of removal and deposition of particles for different periods of the simulation for different density ratio ρ_p/ρ_f at heated and non-heated cavity with *AR* = 1. Generally, the rate of particles removal recorded higher at the early stage of flow development. The percentages of particles removal increase from 0 to 22% at τ = 0 to 10 for ρ_p/ρ_f = 2.0 for non-heated cavity before no particles have been removed for $\tau > 10$. There are slight differences between heated cavity cases. The percentages of particles removed just 20% but at τ = 0 to 9, slightly faster than the non-heated cavity. On the other hand, the percentages of particles removed are 17% and 14% at but at τ = 0 to 7 and τ = 0 to 3 for ρ_p/ρ_f = 5.0 and ρ_p/ρ_f = 10.0 respectively. However, there are no significant differences between heated and non-heated cavity. The rate of particles deposition at the bottom of the cavity is slightly higher at the early stage of flow development before steadily climbing until all the remaining particles settled. For ρ_p/ρ_f = 2.0, the particles deposited increase to 21.8% at τ = 0 to 50 before steadily increase to 41%. As ρ_p/ρ_f increase to 5.0 and 10.0, the rate of particles deposited also increase. The particles deposited increase to 60% at τ = 0 to 50 for ρ_p/ρ_f = 5.0 and

increase to 80% at τ = 0 to 30 for ρ_p/ρ_f = 10.0. When comparing between heated and non-heated cavity, there are no significant differences in trend along time.

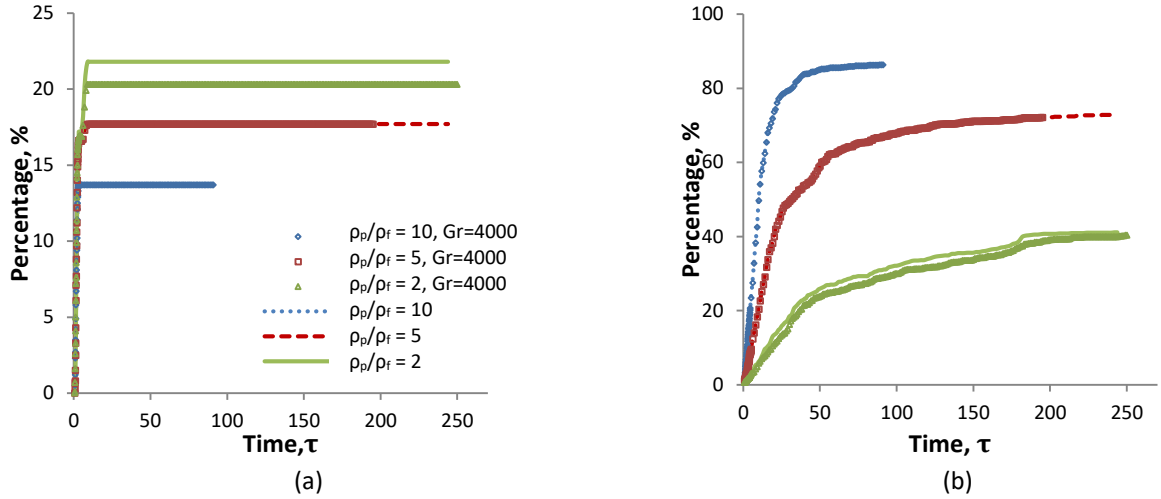

(a) (b)

Fig. 10. Historical comparison of the particles between the heated and non-heated cavity for particles with different density ratio, ρ_p/ρ_f (a) removal of the particles from the cavity and (b) particles deposition at the bottom of the cavity

Interesting remark for particles with ρ_p/ρ_f = 2.0 and 5.0, removal percentage is higher at the early stage of flow development before no longer particles being removed at τ = 9 for ρ_p/ρ_f = 5.0 and $\tau \approx$ 36 for ρ_p/ρ_f = 2.0 as illustrate in Figure 11(a) and (d). After that period, the number of particles deposited exceeds the number of particles being removed. As the density of the particle increases, the removal of particles decreases while deposition percentage was shown increases as illustrated in Figure 12. Generally, there are no significant differences between a heated or non-heated cavity in the results presents.

For the cavity, the number of particles removed in the heated cavity is 21.8% while the non-heated cavity is 20.3%, 1.5% difference between the two for ρ_p/ρ_f = 2.0. As the density ratio increase, the percentage of particles removal decreases. Contrarily to the particles with ρ_p/ρ_f = 2.0, particles with ρ_p/ρ_f = 5.0 and 10.0 shows no differences in removal percentage for both heated and non-heated cavity. For particles deposition, the percentage is increasing as the density ratio of the particles increase [24], the opposite trend from particles removal. The non-heated cavity shows the number of particles deposited slightly higher than the heated cavity with 1.5% and 0.8% of differences for ρ_p/ρ_f = 2.0 and 5.0 respectively. However, for particles with higher density ratio, ρ_p/ρ_f = 10.0, no differences recorded between the heated and non-heated cavity for both removal and deposition percentages.

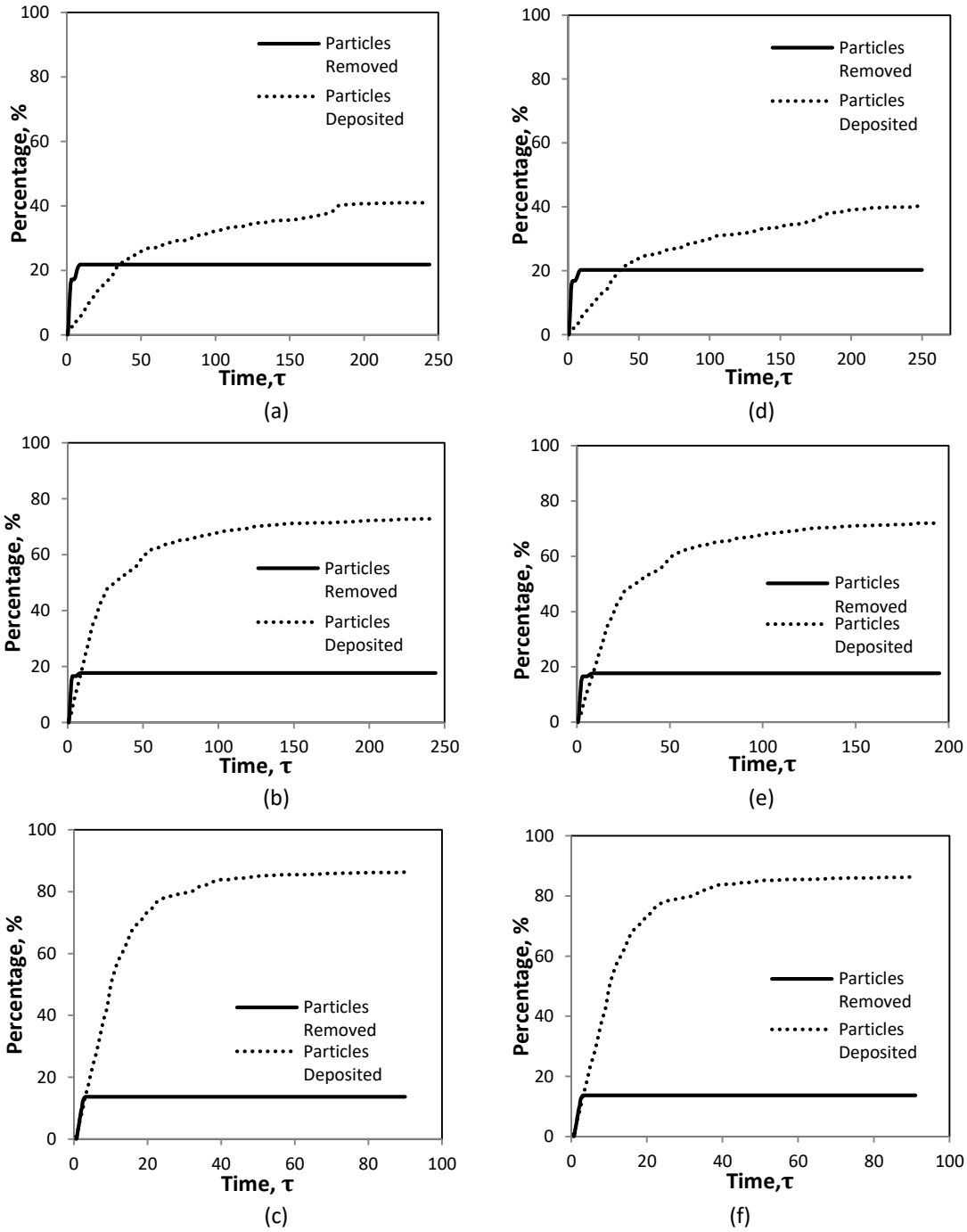

Fig. 11. Percentage of removed and deposited particles on the bottom of the cavity for *AR* = 1 for non-heated cavity at different density ratio, ρ_p/ρ_f, (a) 2.0, (b) 5.0 and (c) 10.0 and heated cavity, *Gr* = 4000 for ρ_p/ρ_f (d) 2.0, (e) 5.0 and (f) 10.0

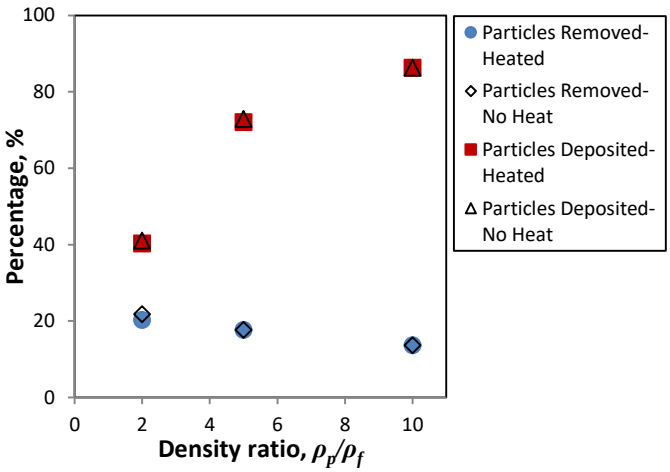

Fig. 12. Percentage of particles removal and deposition for different density ratio, ρ_p/ρ_f for a cavity with *AR* = 1

4. Conclusions

In the present study, it was shown that the flow characteristics change with the influence of the heat presence. In the present research, convection heat transfer occurred either naturally or forcibly dominated. For Re = 50, natural convection dominated and buoyancy forces are larger compared to the inertial force. As a result, the force changes the structure of the flow inside the cavity. As Gr increases from 1000 to 4000, the changes become significant. However, at Re = 1000, the effect of heat is insignificant to the changes of the flow structure inside the cavity as the inertial force from the flow is dominating compared to the buoyancy forces from the heat transfer.

The qualitative study of the behaviour of the particles in present results shows that the particles are dependent on the flow characteristics inside the cavity. The results of the present research also indicate particles with density ratio, ρ_p/ρ_f = 1.0 and 2.0 are easily affected by the flow field in the cavity compared to particles with ρ_p/ρ_f = 5.0 and 10.0. As for particles with ρ_p/ρ_f = 2.0 and 5.0, there are hardly affected by the vertical flow field resulting from inertial forces from the particles themselves. Therefore, the particles tend to drag down and settle due to the gravitational force occurred.

Acknowledgement
This research was not funded by any grant.

References
[1] Yabe, Takashi, and Eiji Takei. "A new higher-order Godunov method for general hyperbolic equations." *Journal of the Physical Society of Japan* 57, no. 8 (1988): 2598-2601. https://doi.org/10.1143/JPSJ.57.2598

[2] Takewaki, H., A. Nishigushi, and T. Yabe. "Cubic interpolated pseudo-particle method (CIP) for solving hyperbolic type equation." *National Institute for Fusion Science. NII-Electronic Library Services* (1985). https://doi.org/10.1016/0021-9991(85)90085-3

[3] Takewaki, Hideaki, and Takashi Yabe. "The cubic-interpolated pseudo particle (CIP) method: application to nonlinear and multi-dimensional hyperbolic equations." *Journal of Computational Physics* 70, no. 2 (1987): 355-372. https://doi.org/10.1016/0021-9991(87)90187-2

[4] Yabe, Takashi, and T. Aoki. "A universal solver for hyperbolic equations by cubic-polynomial interpolation I. One-dimensional solver." *Computer physics communications* 66, no. 2-3 (1991): 219-232. https://doi.org/10.1016/0010-4655(91)90071-R

[5] Ishikawa, T., P. Y. Wang, T. Aoki, Y. Kadota, and F. Ikeda. "A universal solver for hyperbolicequations by cubic-polynomial interpolation. 2. 2-dimensional and 3-dimensional solvers." *Comput. Phys. Commun* 66 (1991): 233-242.
https://doi.org/10.1016/0010-4655(91)90072-S

[6] Shi, YuFeng, Biao Xu, and Yan Guo. "A compact-type CIP method for general Korteweg-de Vries equation." In *Abstract and Applied Analysis*, vol. 2014. Hindawi, 2014.
https://doi.org/10.1155/2014/640194

[7] Xiao, Feng, and Akio Ikebata. "An efficient method for capturing free boundaries in multi-fluid simulations." *International journal for numerical methods in fluids* 42, no. 2 (2003): 187-210.
https://doi.org/10.1002/fld.499

[8] Sato, Yohei, and Bojan Ničeno. "A conservative local interface sharpening scheme for the constrained interpolation profile method." *International Journal for Numerical Methods in Fluids* 70, no. 4 (2012): 441-467.
https://doi.org/10.1002/fld.2695

[9] Nakayama, K. "Comparisons of CIP, compact and CIP-CSL2 schemes for reproducing internal solitary waves." *International Journal for Numerical Methods in Fluids* 51, no. 2 (2006): 197-219.
https://doi.org/10.1002/fld.1112

[10] Yabe, Takashi, Feng Xiao, and Takayuki Utsumi. "The constrained interpolation profile method for multiphase analysis." *Journal of Computational physics* 169, no. 2 (2001): 556-593.
https://doi.org/10.1006/jcph.2000.6625

[11] Toda, Kunihiko, Youichi Ogata, and Takashi Yabe. "Multi-dimensional conservative semi-Lagrangian method of characteristics CIP for the shallow water equations." *Journal of computational physics* 228, no. 13 (2009): 4917-4944.
https://doi.org/10.1016/j.jcp.2009.04.003

[12] Akoh, Ryosuke, Satoshi Ii, and Feng Xiao. "A CIP/multi-moment finite volume method for shallow water equations with source terms." *International journal for numerical methods in fluids* 56, no. 12 (2008): 2245-2270.
https://doi.org/10.1002/fld.1616

[13] Yabe, T., K. Takizawa, M. Chino, M. Imai, and C. C. Chu. "Challenge of CIP as a universal solver for solid, liquid and gas." *International journal for numerical methods in fluids* 47, no. 6-7 (2005): 655-676.
https://doi.org/10.1002/fld.830

[14] Yabe, T., Y. Ogata, K. Takizawa, T. Kawai, A. Segawa, and K. Sakurai. "The next generation CIP as a conservative semi-Lagrangian solver for solid, liquid and gas." *Journal of computational and applied mathematics* 149, no. 1 (2002): 267-277.
https://doi.org/10.1016/S0377-0427(02)00535-6

[15] Tachioka, Yuuki, Yosuke Yasuda, and Tetsuya Sakuma. "Application of the constrained interpolation profile method to room acoustic problems: Examination of boundary modeling and spatial/time discretization." *Acoustical Science and Technology* 33, no. 1 (2012): 21-32.
https://doi.org/10.1250/ast.33.21

[16] Sawada, Kazuhide, Shuji Moriguchi, Atsushi Yashima, Feng Zhang, and Ryosuke Uzuoka. "Large deformation analysis in geomechanics using CIP method." *JSME International Journal Series B Fluids and Thermal Engineering* 47, no. 4 (2004): 735-743.
https://doi.org/10.1299/jsmeb.47.735

[17] Moriguchi, Shuji, Atsushi Yashima, Kazuhide Sawada, Ryosuke Uzuoka, and Masatoshi Ito. "Numerical simulation of flow failure of geomaterials based on fluid dynamics." *Soils and Foundations* 45, no. 2 (2005): 155-165.
https://doi.org/10.3208/sandf.45.2_155

[18] Yokoi, Kensuke, Feng Xiao, Hao Liu, and Kazuaki Fukasaku. "Three-dimensional numerical simulation of flows with complex geometries in a regular Cartesian grid and its application to blood flow in cerebral artery with multiple aneurysms." *Journal of computational physics* 202, no. 1 (2005): 1-19.
https://doi.org/10.1016/j.jcp.2004.06.018

[19] Takizawa, Kenji, Takashi Yabe, Minoru Chino, Takao Kawai, Kei Wataji, Hideaki Hoshino, and Takeshi Watanabe. "Simulation and experiment on swimming fish and skimmer by CIP method." *Computers & structures* 83, no. 6-7 (2005): 397-408.
https://doi.org/10.1016/j.compstruc.2004.04.023

[20] Ida, Masato. "An improved unified solver for compressible and incompressible fluids involving free surfaces. Part I. Convection." *Computer Physics Communications* 132, no. 1-2 (2000): 44-65.
https://doi.org/10.1016/S0010-4655(00)00136-3

[21] Azwadi, Nor, A. S. Ahmad Sofianuddin, and K. Y. Ahmat Rajab. "Transient Removal of Contaminants in Cavity of Mixed Convection in a Channel by Constrained Interpolated Profile Method." *Applied Mechanics & Materials* 554 (2014).
https://doi.org/10.4028/www.scientific.net/AMM.554.312

[22] Sheldareh, Ali Akbari, Arman Safdari, and Nor Azwadi Che Sidik. "Numerical prediction of heat transfer from localized heating in enclosure using CIP method." In *Applied Mechanics and Materials*, vol. 315, pp. 512-516. Trans Tech Publications Ltd, 2013.
https://doi.org/10.4028/www.scientific.net/AMM.315.512

[23] Kosinski, Pawel, Anna Kosinska, and Alex Christian Hoffmann. "Simulation of solid particles behaviour in a driven cavity flow." *Powder Technology* 191, no. 3 (2009): 327-339.

[24] Safdari, Arman, and Kyung Chun Kim. "Lattice Boltzmann simulation of solid particles behavior in a three-dimensional lid-driven cavity flow." *Computers & Mathematics with Applications* 68, no. 5 (2014): 606-621.
https://doi.org/10.1016/j.camwa.2014.07.004

[25] Pratsinis, Sotiris E., and Kyo-Seon Kim. "Particle coagulation, diffusion and thermophoresis in laminar tube flows." *Journal of Aerosol Science* 20, no. 1 (1989): 101-111.
https://doi.org/10.1016/0021-8502(89)90034-7

[26] Patankar, N. A., and D. D. Joseph. "Modeling and numerical simulation of particulate flows by the Eulerian–Lagrangian approach." *International Journal of Multiphase Flow* 27, no. 10 (2001): 1659-1684.
https://doi.org/10.1016/S0301-9322(01)00021-0

[27] Saadun, Mohd Noor Asril, C. S. Azwadi, M. N. Hazwani, Mohamad Shukri Zakaria, Muhammad Zaidan Abdul Manaf, Mohd Hanafi, and Mohd Hafidzal. "Numerical analysis on the effects of cavity geometry with heat towards contaminant removal." In *Applied Mechanics and Materials*, vol. 393, pp. 851-856. Trans Tech Publications Ltd, 2013.
https://doi.org/10.4028/www.scientific.net/AMM.393.851

[28] Sidik, Nor Azwadi Che, and Mehran Salehi. "Eulerian–Lagrangian numerical scheme for contaminant removal from different cavity shapes." *Arabian Journal for Science and Engineering* 39, no. 4 (2014): 3181-3189.
https://doi.org/10.1007/s13369-013-0886-5

[29] He, Chunhong, and Goodarz Ahmadi. "Particle deposition with thermophoresis in laminar and turbulent duct flows." *Aerosol science and technology* 29, no. 6 (1998): 525-546.
https://doi.org/10.1080/02786829808965588

[30] Akbar, M. K., M. Rahman, and S. M. Ghiaasiaan. "Particle transport in a small square enclosure in laminar natural convection." *Journal of Aerosol Science* 40, no. 9 (2009): 747-761.
https://doi.org/10.1016/j.jaerosci.2009.04.007

[31] Haeri, S., and J. S. Shrimpton. "Fully resolved simulation of particle deposition and heat transfer in a differentially heated cavity." *International journal of heat and fluid flow* 50 (2014): 1-15.
https://doi.org/10.1016/j.ijheatfluidflow.2014.04.009

[32] Jahanshaloo, Leila, Nor Azwadi Che Sidik, Shahin Salimi, and Arman Safdari. "The use of thermal lattice Boltzmann numerical scheme for particle-laden channel flow with a cavity." *Numerical Heat Transfer, Part A: Applications* 66, no. 4 (2014): 433-448.
https://doi.org/10.1080/10407782.2014.884898

[33] Feng, Zhi-Gang, and Efstathios E. Michaelides. "Inclusion of heat transfer computations for particle laden flows." *Physics of Fluids* 20, no. 4 (2008): 040604.
https://doi.org/10.1063/1.2911022

[34] Chilukuri, Radhakrishna, and Stanley Middleman. "Circulation, diffusion, and reaction within a liquid trapped in a cavity." *Chemical Engineering Communications* 22, no. 3-4 (1983): 127-138.
https://doi.org/10.1080/00986448308940051

[35] Fang, L. C., D. Nicolaou, and J. W. Cleaver. "Transient removal of a contaminated fluid from a cavity." *International journal of heat and fluid flow* 20, no. 6 (1999): 605-613.
https://doi.org/10.1016/S0142-727X(99)00050-8

[36] Mickaily, Elizabeth S., and Stanley Middleman. "Hydrodynamic cleaning of a viscous film from the inside of a long tube." *AIChE journal* 39, no. 5 (1993): 885-893.

[37] Alkire, Richard C., David B. Reiser, and Robert L. Sani. "Effect of fluid flow on removal of dissolution products from small cavities." *Journal of the Electrochemical Society* 131, no. 12 (1984): 2795.
https://doi.org/10.1149/1.2115410

[38] TIGHE, STEVEN, and STANLEY MIDDLEMAN. "An experimental study of convection-aided removal of a contaminant from a cavity in a surface." *Chemical Engineering Communications* 33, no. 1-4 (1985): 149-157.
https://doi.org/10.1080/00986448508911166

[39] Alkire, Richard, and Hariklia Deligianni. "The role of mass transport on anisotropic electrochemical pattern etching." *Journal of the Electrochemical Society* 135, no. 5 (1988): 1093. https://doi.org/10.1149/1.2095882
[40] Fang, Lih-Chuan. "Effect of mixed convection on transient hydrodynamic removal of a contaminant from a cavity." *International journal of heat and mass transfer* 46, no. 11 (2003): 2039-2049. https://doi.org/10.1016/S0017-9310(02)00507-0
[41] Fang, Lih-chuan. "Effect of duct velocity profile and buoyancy-induced flow on efficiency of transient hydrodynamic removal of a contaminant from a cavity." *International journal for numerical methods in fluids* 44, no. 12 (2004): 1389-1404. https://doi.org/10.1002/fld.676
[42] Molki, Arman, Lyes Khezzar, and Afshin Goharzadeh. "Measurement of fluid velocity development in laminar pipe flow using laser Doppler velocimetry." *European Journal of Physics* 34, no. 5 (2013): 1127. https://doi.org/10.1088/0143-0807/34/5/1127
[43] Smits, A. J., and Lim, T. T. *Flow visualization: Techniques and examples*. Imperial College Press. ISBN 1-86094-193-1, 2000. https://doi.org/10.1142/p167
[44] Settles, Gary S. *Schlieren and shadowgraph techniques: visualizing phenomena in transparent media*. Springer Science & Business Media, 2012.
[45] Samimy, Mohammad, Kenneth S. Breuer, L. Gary Leal, and Paul H. Steen, eds. "A gallery of fluid motion." (2004): 1262-1263. https://doi.org/10.1119/1.1778399
[46] Mega, Eduardo F., Vinicius S. Morais, Edson DR Vieira, and Sérgio S. Mansur. "EXPERIMENTAL VISUALIZATION OF THE FLOW INSIDE OPEN CAVITIES." (2007).
[47] Yabe, Takashi. "A universal cubic interpolation solver for compressible and incompressible fluids." *Shock Waves* 1, no. 3 (1991): 187-195. https://doi.org/10.1007/BF01413793
[48] A. Sahak, Ahmad Sofianuddin. "Cubic Interpolation Pseudo-Particle Navier-Stokes Formulation Method for Particle-Fluid Interaction in Cavity." PhD diss., Universiti Teknologi Malaysia, 2020.
[49] Zhu, H. P., Z. Y. Zhou, R. Y. Yang, and A. B. Yu. "Discrete particle simulation of particulate systems: theoretical developments." *Chemical Engineering Science* 62, no. 13 (2007): 3378-3396. https://doi.org/10.1016/j.ces.2006.12.089
[50] Crowe, Clayton T., John D. Schwarzkopf, Martin Sommerfeld, and Yutaka Tsuji. *Multiphase flows with droplets and particles*. CRC press, 2011.
[51] Tsorng, S. J., H. Capart, J. S. Lai, and D. L. Young. "Three-dimensional tracking of the long time trajectories of suspended particles in a lid-driven cavity flow." *Experiments in Fluids* 40, no. 2 (2006): 314-328. https://doi.org/10.1007/s00348-005-0070-0
[52] Manca, Oronzio, Sergio Nardini, Khalil Khanafer, and Kambiz Vafai. "Effect of heated wall position on mixed convection in a channel with an open cavity." *Numerical Heat Transfer: Part A: Applications* 43, no. 3 (2003): 259-282. https://doi.org/10.1080/10407780307310
[53] Abdelmassih, Gorg, Anton Vernet, and Jordi Pallares. "Steady and unsteady mixed convection flow in a cubical open cavity with the bottom wall heated." *International Journal of Heat and Mass Transfer* 101 (2016): 682-691. https://doi.org/10.1016/j.ijheatmasstransfer.2016.05.074
[54] Stiriba, Y. F. J. A., J. A. Ferré, and F. X. Grau. "Heat transfer and fluid flow characteristics of laminar flow past an open cavity with heating from below." *International Communications in Heat and Mass Transfer* 43 (2013): 8-15. https://doi.org/10.1016/j.icheatmasstransfer.2013.01.010
[55] Brandon, Daniel J., and S. K. Aggarwal. "A numerical investigation of particle deposition on a square cylinder placed in a channel flow." *Aerosol Science & Technology* 34, no. 4 (2001): 340-352. https://doi.org/10.1080/02786820121279
[56] Jafari, Saeed, Mazyar Salmanzadeh, Mohammad Rahnama, and Goodarz Ahmadi. "Investigation of particle dispersion and deposition in a channel with a square cylinder obstruction using the lattice Boltzmann method." *Journal of Aerosol Science* 41, no. 2 (2010): 198-206.